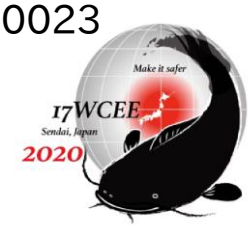

17th World Conference on Earthquake Engineering, 17WCEE
Sendai, Japan - September 13th to 18th 2020

DIMENSIONAL ANALYSIS OF SEISMIC RESPONSES OF ROCKING WALL-FRAME STRUCTURES

Dixiong Yang [1], Guiqiang Guo [2]

[1] *Professor, Department of Engineering Mechanics, Dalian University of Technology, State Key Laboratory of Structural Analysis for Industrial Equipment, Dalian 116024, China, Email: yangdx@dlut.edu.cn*
[2] *Doctor, Department of Engineering Mechanics, Dalian University of Technology, State Key Laboratory of Structural Analysis for Industrial Equipment, Dalian 116024, China, Email: guo.gq@outlook.com*

Abstract

The rocking wall-frame structures are attracting more and more attention from the community of earthquake engineering, owing to the advantage of avoiding the weak-story failure mechanism and hence of global failure mechanism. To further suppress the structural response and to achieve a self-centering function, a number of supplemental control devices are proposed to improve the seismic performance of the pure dual system of frame and rocking wall. These devices can be divided into two kinds in terms of mechanical mechanism, concentrated control device CCD (e.g., rotational spring) applied on the base of the rocking wall and distributed control device DCD (e.g., damper) on the entire structural height. It should be noted that some works indeed utilized these two kinds of devices at the same time. Nevertheless, there is no systematical study on the influences of these two kinds of devices on the dual system and on whether it is necessary to simultaneously used them or not. Thus, the effect of vibration control by CCD and DCD on the rocking wall-frame structures is systematically compared. Particularly, the widely adopted flexural-shear beam is utilized to represent the rocking wall-frame structures, and the dimensional analysis is also used to carry out a parametric analysis. The vibration characteristics and static responses of the flexural-shear beam with two devices are first examined in this paper. Results indicates that the fundamental period of the flexural-shear beam clearly decreases with increasing DCD, that the base moment resisted by the rocking wall remarkably increases with strengthening CCD, and that both these two devices lead to a notable increase in the base shear resisted by the rocking wall. Furthermore, the dynamic response analysis of the flexural-shear beam is implemented in both cases of idealized pulses and near-fault pulse-like ground motions. It is shown that the DCD generally can sufficiently suppress the interstory drift of the flexural-shear beam but cause a significant drift concentration, while the CCD does not sufficiently reduce the drift yet clearly avoids drift concentration. Additionally, in the case of ground motion records both devices are generally detrimental for the control of floor acceleration response. Therefore, the appropriate devices utilized in practical seismic design should be determined in accordance with the structural responses of interest.

Keywords: Rocking wall-frame structures; Dimensional analysis; Flexural-shear beam; Vibration control

1. Introduction

As a promising seismic design philosophy, rocking isolation is attracting more and more attention from the community of earthquake engineering [1−4]. It is recognized that the main advantage of rocking structures is to dissipate the input energy by ground motions via rocking response, and hence the structures suffer minor or no damage during strong earthquakes. To reduce the interstory drift demands of moment-resisting frame structures, the stepping rocking wall and pinned rocking wall are proposed to replace the fixed-base wall in a conventional wall-frame structure [5, 6]. Generally, both stepping and pinned rocking walls can suppress the interstory drift responses of building structures. In fact, Diamantopoulos and Fragiadakis [7] showed that stepping rocking structures can be modeled as equivalent pinned rocking structures with rotational spring at the base. To further improve seismic performance and reduce global displacement, supplemental control devices are essential to form rocking wall-frame building structures with self-centering capacity. The control devices available in the literature can be classified as: (a) concentrated control device (CCD) causing a concentrated constraint, e.g., precast tendons to anchor the rocking wall to ground [5]; (b) distributed control device (DCD) causing a distributed constraint, e.g., dampers equipped between the rocking wall and frame over the entire building height [8]. Particularly, these two kinds of control devices are utilized together by Grigorian and his co-workers [9−11] in the preliminary design of rocking wall-frames structures. Nevertheless, there is currently no published works addressing the following issues, e.g., which control device is better and whether it is necessary to adopt both devices together. To this end, this paper systematically investigates the vibration characteristics and static/dynamic responses of rocking wall-frame structures equipped with CCD and DCD. Particularly, the rocking wall-frame structure is modeled as a flexural-shear beam model [12], wherein the flexural beam is pinned at the base. Correspondingly, CCD and DCD are idealized as the concentrated constraint at the base of the flexural beam [13] and the distributed constraint between the flexural beam and shear beam over entire beam height [14], respectively.

2. Flexural-shear beam model for rocking wall-frame structures

It can be seen from Fig.1 that the precast tendon is utilized to anchor the stepping rocking wall to ground (Fig. 1A) and the dampers are equipped between the pinned rocking wall and frame (Fig. 1B). It should be noted that the dampers at different floors are identical. As shown in Fig. 1C, the rocking wall-frame structure equipped with these two devices can be modeled as a flexural-shear beam with concentrated and distributed constraints.

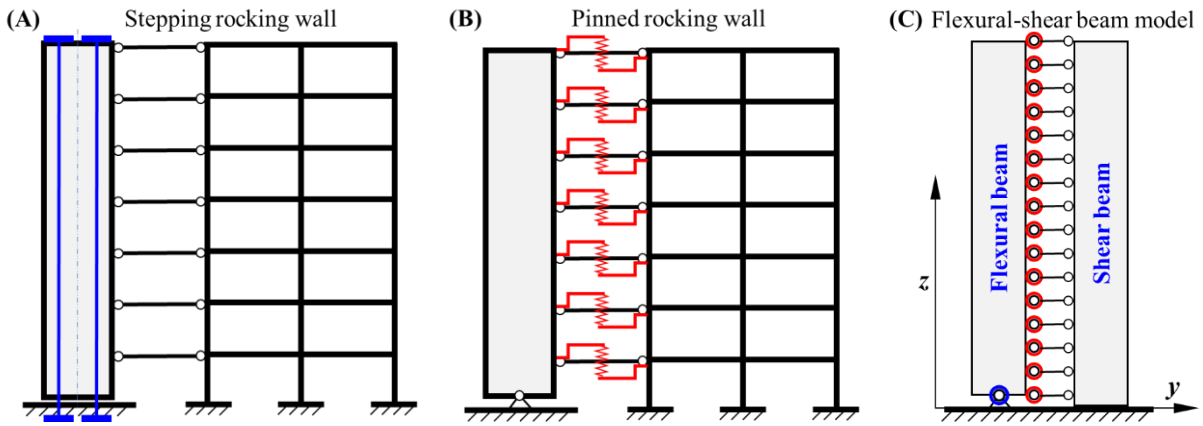

Fig. 1 – Rocking wall-frame structure: (A) stepping rocking wall & precast tendons (B) pinned rocking wall & dampers (C) flexural-shear beam model with concentrated and distributed constraints

According to Miranda [12] and Sun et al. [14], the lateral displacement response of the undamped uniform continuous beam model subjected to a ground acceleration $\ddot{u}_g(t)$ is given by the following partial differential equation

$$\frac{\rho}{EI}\frac{\partial^2 u(x,t)}{\partial t^2}+\frac{1}{H^4}\frac{\partial^4 u(x,t)}{\partial x^4}-\frac{\bar{\alpha}^2}{H^4}\frac{\partial^2 u(x,t)}{\partial x^2}=-\frac{\rho}{EI}\frac{\partial^2 u_g(t)}{\partial t^2} \tag{1}$$

where ρ denotes the mass per length, EI indicates the flexural stiffness, H represents the height of flexural-shear beam, GA is the shear stiffness, G_dA_d means the equivalent shear stiffness of DCD, and $u(x, t)$ is the lateral displacement at nondimensional height $x = z/H$ at time t, $\lambda = G_dA_d/GA$ is denoted as the distributed constraint parameter of DCD, and $\bar{\alpha}=H\sqrt{\frac{(1+\lambda)GA}{EI}}=\alpha\sqrt{1+\lambda}$. For rocking wall-frame building structures, the lateral stiffness ratio α ranges from 1.5 to 6 [12], while the distributed constraint parameter λ generally lies in the region of [0, 1] [14].

3. Dimensional analysis of flexural-shear beam model

Dimensional analysis is widely used in the seismic response analysis of engineering structures, since it was firstly introduced into earthquake engineering in 2004 [15−18]. To examine the influences of control devices on the vibration characteristics and static/dynamic responses of flexural-shear beams, this paper adopts dimensional analysis to unveil the inherent order of seismic responses and to effectively implement parameter analysis.

3.1 MP pulse model

Many idealized pulse models have been proposed to deeply investigate the impulsive features of near-fault pulse-like ground motions and to synthesize stochastic ground motions. Among those is the MP pulse model that can fully characterizes the key features of near-fault pulse-like ground motions [19, 20]. The velocity pulse of the MP pulse model can be expressed as

$$\dot{u}_g^{\mathrm{MP}}(t)=\frac{v_0}{2}\left[1-\cos\left(\frac{\omega_p}{\gamma}t\right)\right]\cos\left(\omega_p t-\pi\gamma+\varphi\right)\quad\left(0\le t\le\gamma T_p,\ \gamma>1\right) \tag{2}$$

where φ and ω_p are the phase and circular frequency of the amplitude-modulated harmonic in Eq. (2) respectively, while v_0 and γ separately defines the amplitude and oscillatory character of the MP velocity pulse. It is obvious that different pairs of γ and φ simulate different types of MP pulses. The acceleration amplitude of the fling-step pulse ($\gamma = 1.01$, $\varphi = 0$) is $a_p \approx 0.879\omega_p v_0$, whereas that of the forward-directivity pulse ($\gamma = 1.01$, $\varphi = \pi/2$) is $a_p \approx \omega_p v_0$. For convenience, the MP pulse can be simply expressed as $\ddot{u}_g^{\mathrm{MP}}\left(a_p,\omega_p,\gamma,\varphi\right)$.

3.2 Dimensional analysis

Obviously, the fundamental period depends on structural parameters, including shear stiffness GA, flexural stiffness EI, linear density ρ, building height H, equivalent shear stiffness of dampers G_dA_d and rotational spring stiffness K_r. Thus, the fundamental period T_1 can be written as

$$T_1=\bar{f}_1\left(GA,EI,\rho,H,G_dA_d,K_r\right) \tag{3}$$

According to Buckingham's Π-theorem, select EI, ρ and H as parameters with independent dimensions, and Eq. (3) can be reduced to

$$T_1\sqrt{\frac{EI}{\rho H^4}}=\bar{\Phi}_1\left(H^2\frac{GA}{EI},H^2\frac{G_dA_d}{EI},\frac{K_rH}{EI}\right)=\bar{\Phi}_1\left(\alpha^2,\lambda\alpha^2,R_f\right)=\Phi_1\left(\alpha,\lambda,R_f\right) \tag{4}$$

Furthermore, the seismic responses considered herein include the maximum interstory drift ratio MIDR, maximum floor acceleration MFA and drift concentrated factor DCF. The three seismic responses of the flexural-shear beam subjected to MP pulses can be expressed mathematically as

$$\begin{aligned}\text{MIDR} &= \bar{f}_2\left(GA, EI, \rho, H, G_\text{d}A_\text{d}, K_\text{r}, \xi, a_\text{p}, \omega_\text{p}, \gamma, \varphi\right)\\ \text{MFA} &= \bar{f}_3\left(GA, EI, \rho, H, G_\text{d}A_\text{d}, K_\text{r}, \xi, a_\text{p}, \omega_\text{p}, \gamma, \varphi\right)\\ \text{DCF} &= \bar{f}_4\left(GA, EI, \rho, H, G_\text{d}A_\text{d}, K_\text{r}, \xi, a_\text{p}, \omega_\text{p}, \gamma, \varphi\right)\end{aligned} \tag{5}$$

Similarly, according to Buckingham's Π-theorem, Eq. (5) can be reduced to

$$\begin{aligned}\text{MIDR} &= \bar{\Phi}_2\left(H^2\frac{GA}{EI}, H^2\frac{G_\text{d}A_\text{d}}{EI}, \frac{K_\text{r}H}{EI}, a_\text{p}\frac{\rho H^3}{EI}, \omega_\text{p}\sqrt{\frac{\rho H^4}{EI}}, \xi, \gamma, \varphi\right) = \bar{\Phi}_2\left(\alpha^2, \lambda\alpha^2, R_\text{f}, a_\text{p}\frac{\beta^2}{H}, \omega_\text{p}\beta, \xi, \gamma, \varphi\right)\\ \text{MFA}\frac{\rho H^3}{EI} &= \bar{\Phi}_3\left(H^2\frac{GA}{EI}, H^2\frac{G_\text{d}A_\text{d}}{EI}, \frac{K_\text{r}H}{EI}, a_\text{p}\frac{\rho H^3}{EI}, \omega_\text{p}\sqrt{\frac{\rho H^4}{EI}}, \xi, \gamma, \varphi\right) = \bar{\Phi}_3\left(\alpha^2, \lambda\alpha^2, R_\text{f}, a_\text{p}\frac{\beta^2}{H}, \omega_\text{p}\beta, \xi, \gamma, \varphi\right)\\ \text{DCF} &= \bar{\Phi}_4\left(H^2\frac{GA}{EI}, H^2\frac{G_\text{d}A_\text{d}}{EI}, \frac{K_\text{r}H}{EI}, a_\text{p}\frac{\rho H^3}{EI}, \omega_\text{p}\sqrt{\frac{\rho H^4}{EI}}, \xi, \gamma, \varphi\right) = \bar{\Phi}_4\left(\alpha^2, \lambda\alpha^2, R_\text{f}, a_\text{p}\frac{\beta^2}{H}, \omega_\text{p}\beta, \xi, \gamma, \varphi\right)\end{aligned} \tag{6}$$

4. Influences of control devices on the vibration characteristics and static/dynamic responses of rocking wall-frame buildings

4.1. Vibration characteristics

This part aims to investigate examine the influences of control devices on the vibration characteristics of rocking wall-frame building structures via the flexural-shear beam model. Firstly, the fundamental period is examined according to the relationship between the fundamental period and structural parameters in the previous section.

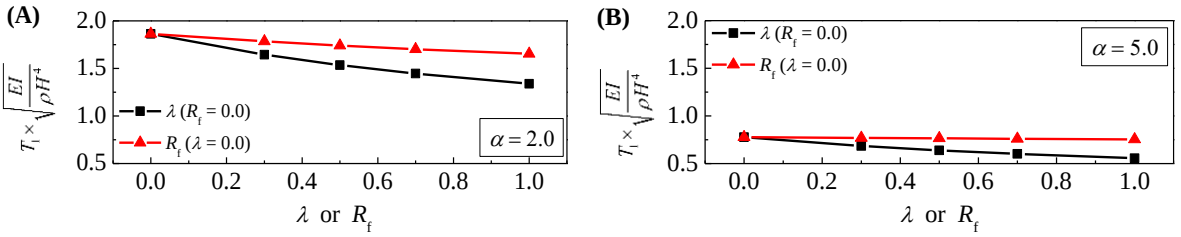

Fig. 2 – Influences of control devices on the normalized fundamental period of flexural-shear beam

Fig. 2 demonstrates that the influences of control devices on the normalized fundamental period of the flexural-shear beam, in which λ = 0 means no dampers between rocking wall and frame, and R_f = 0 indicates no precast tendons to anchor the rocking wall. The fundamental period decreases with increasing constraint parameters, especially for distributed constraint parameter λ. Note that decreasing fundamental period implies increasing lateral stiffness. For rocking wall-frame buildings with fundamental-mode dominated response, it is deduced that DCD can much more effectively suppress the interstory drift demand than CCD.

On the other hand, the mode shape and its derivative are also the main aspects of vibration characteristics, and hence are considered herein. Note that the modal participation factor depends on how the mode shapes are normalized, whereas the product of modal participation factor and mode shape (or mode shape derivative) is independent of how the mode shapes are normalized [12]. Thus, the product of modal participation factor and mode shape (or mode shape derivative) for the fundamental mode is examined. It can be seen from Fig. 3 that both control devices impose negligible influences on the product of the fundamental mode shape and its modal participation factor of the flexural-shear beam. This implies that both control devices do not change

the rocking mode of the rocking wall-frame buildings, and both constraint parameters (λ and R_f) hence lie in a reasonable region.

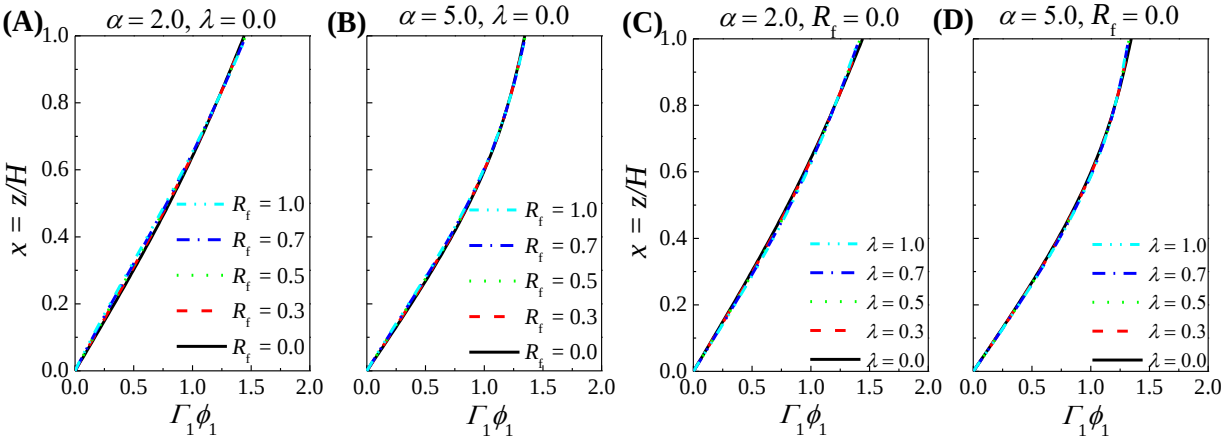

Fig. 3 – Influences of control devices on the product of the mode shape and its modal participation factor of flexural-shear beam

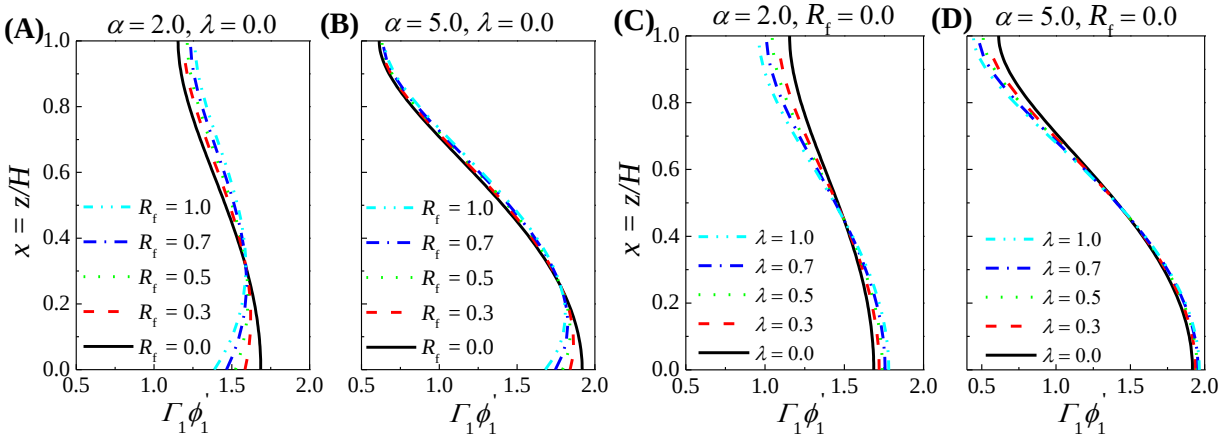

Fig. 4 – Influences of control devices on the product of the mode shape derivative and its modal participation factor of flexural-shear beam

Fig. 4 furthermore indicates the influences of control devices on the product of the fundamental mode shape derivative and its modal participation factor of the flexural-shear beam. It is observed from Fig. 4A–B that the normalized mode shape derivative increases with increasing concentrated constraint parameter R_f in the upper two-thirds of building height, yet decreases with increasing R_f in the lower one-third of building height. In contrast, Fig. 4C–D indicates that the normalized mode shape derivative decreases with increasing distributed constraint parameter λ in the upper half of building height, but increases with increasing λ in the lower half of building height. The above opposite trends imply that CCD would lead to a more uniform distribution of drift response, whereas DCD would result in drift concentration.

4.2. Static responses to inverted triangle lateral loads

This subsection focuses on the static responses to inverted triangle lateral loads $p_t(z) = q_t z/H$ that characterize ground motions in seismic design. In detail, the normalized shear force and moment resisted by the rocking wall and the interstory drift response are considered herein.

Firstly, Fig. 5 illustrates that the effects of control devices on the shear force resisted by the rocking wall, where the shear force is normalized with respect to the base shear $V_0 = 0.5q_tH$. Note that the shear force changes sign over the wall height, which is attributed to the interaction of the rocking wall and the frame. It

can be seen from Fig. 5A–B that the implementation of CCD at the base of the rocking wall leads to a clear increase in the shear force at the bottom, yet a slight decrease in the shear force at the top. Obviously, this influence is closely related to the physical location of the CCD. While Fig. 5C–D indicates that DCD imposes similar influences on the shear force, but the changes at the top and bottom are basically uniform. Thus, compared with CCD, DCD is more effective to change the shear force resisted by the rocking wall.

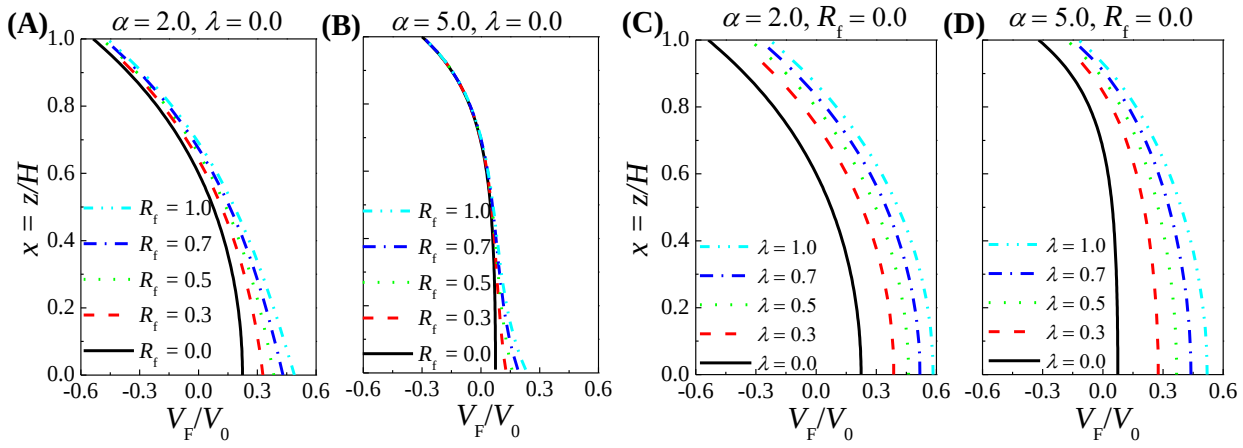

Fig. 5 – Influences of control devices on the shear force resisted by the rocking wall

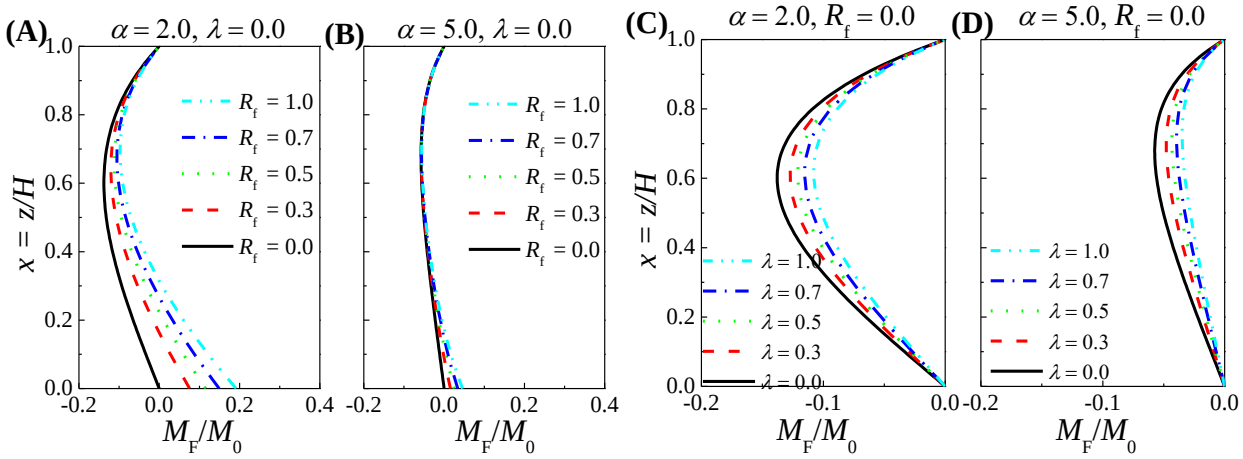

Fig. 6 – Influences of control devices on the moment resisted by the rocking wall

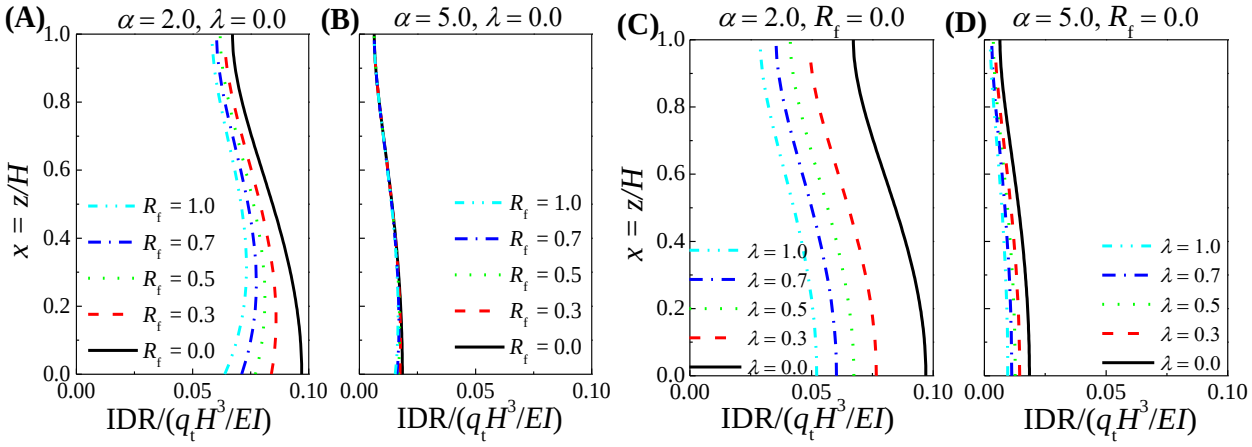

Fig. 7 – Influences of control devices on the interstory drift of flexural-shear beam

Furthermore, Fig. 6 depicts the influences of control devices on the moment resisted by the rocking wall, where the moment is normalized with respect to the base moment $M_0 = (1/3)q_t H^2$. Fig. 6A–B indicates that the implementation of CCD at the base of the rocking wall leads to a clear increase in the moment at the bottom, yet a slight decrease in the shear force at the upper part. Whereas, Fig. 6C–D shows that DCD can reduce the moment but does not change the distribution of the moment. Fig. 7A–B indicates that CCD reduces the interstory drift response especially that at the bottom of the flexural-shear beam. However, it can be seen from Fig. 7C–D that DCD can significantly suppress the interstory drift response along the whole height. Additionally, the decreases in the drift at the bottom and top basically equal each other. In fact, it is shown earlier that DCD can significantly reduce the fundamental period of the flexural-shear beam, i.e., increasing the lateral stiffness. Accordingly, the interstory drift response can be effectively suppressed by DCD when subjected to inverted triangle lateral loads.

4.3. Dynamic responses to MP pulses and near-fault ground motions

To analyze the control effect of control devices, namely CCD and DCD, the forward-directivity pulse simulated by the MP pulse model [19, 21] are first input to the flexural-shear beam. In addition, the frequency ratio considerably affects the dimensionless dynamic responses of the flexural-shear beam. Thus, three frequency ratios, $\Pi_{\omega,p1}$ = 0.5, 1.0 and 2.0, are considered herein, designated as low-, intermediate- and high-frequency pulses, respectively.

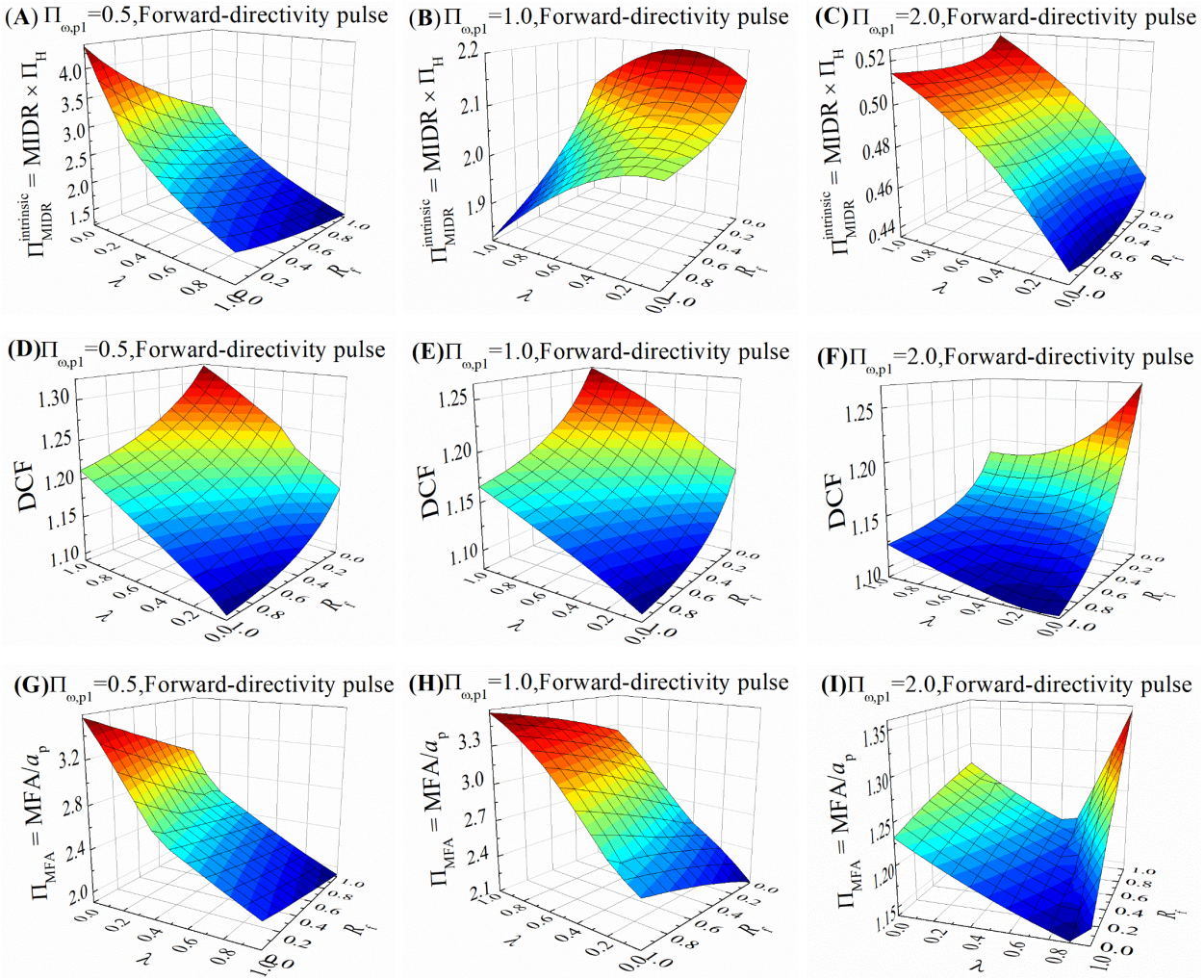

Fig. 8 − Influences of control devices on normalized seismic responses of the flexural-shear beam subjected to forward-directivity pulses

Fig. 8 displays the influences of control devices on the seismic responses of the flexural-shear beam subjected to forward-directivity pulses. As shown in Fig. 8A corresponding to low-frequency pulses, the interstory drift decreases with increasing parameters λ and R_f, especially for the parameter λ, which is in consistent with the previous results in Fig. 7. Fig. 8B indicates that in the case of intermediate-frequency pulses increasing parameters λ and Rf generally suppresses the interstory drift response, and the control effect is considerably significant when CCD and DCD are utilized together. However, Fig. 8C shows that the interstory drift response is almost unchanged with increasing parameter R_f. Particularly, increasing parameter λ results in larger interstory drift responses, a counterintuitive situation. That is to say, both CCD and DCD cannot suppress the interstory drift response for the case of high-frequency pulses. Furthermore, it can be seen from Fig. 8D−E that the drift concentration factor DCF decreases with increasing parameter R_f, yet increases with increasing parameter λ in the cases of low- and intermediate-frequency pulses. This is easy to understand, if note that the opposite influences of parameters λ and R_f on the fundamental mode shape derivative shown in Fig. 4. In the case of high-frequency pulses, Fig. 8F indicates that increasing parameter R_f still reduces DCF, whereas increasing parameter λ suppresses DCF for small R_f yet enlarges DCF for large R_f. From the point of view of avoiding drift concentration, CCD is a reasonable choice. As for the maximum floor acceleration response, it is seen from Fig. 8G associated with low-frequency pulses that the floor acceleration response decreases with increasing parameters λ and R_f, especially for the parameter λ. In contrast, Fig. 8H indicates the floor acceleration response increases with increasing parameters λ and R_f in the case of intermediate-frequency pulses, which implies that both CCD and DCD are detrimental to suppress floor acceleration responses. Additionally, in the case of high-frequency pulses, the floor acceleration response first decreases and then increases with increasing parameter λ, whereas the floor acceleration increases with increasing parameter R_f.

Generally, idealized MP pulses just represent the main impulsive characters of near-fault pulse-like ground motions, do not account for the rich high-frequency contents. This part utilizes one typical near-fault pulse-like ground motions, i.e., record RRS228 from 1994 Northridge, California earthquake which is induced by the forward-directivity effect. For the record RRS228 with distinct acceleration pulse, ground motion parameters (a_p and ω_p) for dimensional analysis are obtained by fitting idealized MP pulse [15, 16]. Similarly, three frequency ratios, 0.5, 1.0 and 2.0, are considered herein, designated as low-, intermediate- and high-frequency ground motions, respectively.

Fig. 9 indicates the influences of control devices on the seismic responses of the flexural-shear beam subjected to ground motion record RRS228 with forward-directivity effect. It can be seen from Fig. 9A−F that the evolution trends of interstory drift and DCF with increasing parameters λ and R_f are basically in consistent with those in Fig. 8A−F associated with forward-directivity pulses. Fig. 9G indicates that the floor acceleration response decreases and then increases with increasing parameter λ, and the influence of R_f obviously depends on the value of parameter λ. Even though, it is feasible to only utilize DCD to suppress the floor acceleration response in the case of low-frequency ground motions. However, as shown in Fig. 9H−I, increasing parameters λ and R_f generally enlarges the floor acceleration response for the cases of intermediate- and high-frequency ground motions. This implies that both CCD and DCD are detrimental to reduce the floor acceleration response.

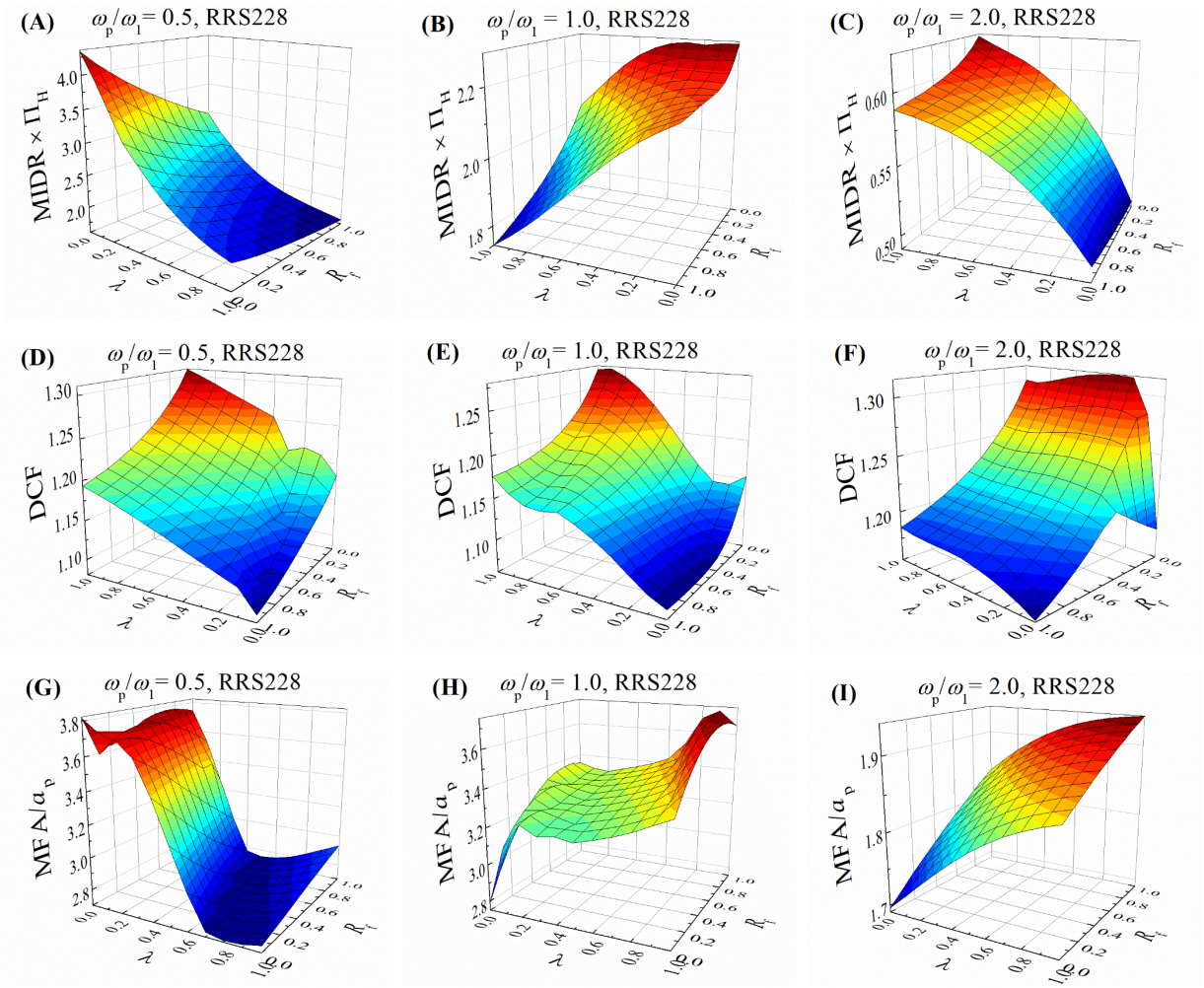

Fig. 9 − Influences of control devices on the seismic responses of the flexural-shear beam subjected to ground motion record RRS228

5. Conclusions

As a promising seismic structural system, the rocking wall-frame building structures are attracting more and more attentions from structural engineers. To further improve seismic performance and suppress global responses, two kinds of control devices (namely CCD and DCD) are installed on the rocking wall-frame buildings to form self-centering seismic structures. This paper systematically investigates the influences of control devices on the rocking wall-frame buildings modeled as flexural-shear beam subjected to near-fault impulsive ground motions, where the control devices are idealized as concentrated and distributed constraints. Through a series of detailed analyses on the vibration characteristics and static responses as well as dimensionless dynamic responses of the flexural-shear beams for rocking wall-frame buildings, several main conclusions are drawn as follows:

(1) Dimensional analysis with intrinsic length scale is utilized to unveil the inherent order of seismic responses and to effectively implement parameter analysis. The normalized seismic responses (i.e., $\Pi_{MIDR}^{intrinsic}$, Π_{MFA} and DCF) present complete self-similarity in the normalized building height and the beauty of order. Hence, the parametric analysis is simplified, while the results are still universal.

(2) DCD clearly reduces the fundamental period of rocking wall-frame buildings (i.e., larger lateral stiffness), while CCD imposes a similar yet marginal influence. In addition, DCD enlarges the nonuniformity of the

fundamental mode shape derivative, whereas CCD reduces it. It should be noted that both devices exert a neglectable effect on the fundamental mode shape.

(3) When the rocking wall-frame buildings are subjected to inverted triangle lateral loads, DCD significantly increases the shear force at the base of rocking wall, and decreases the shear force at the bottom, as well as suppresses the interstory drift of the rocking wall-frame buildings. Particularly, CCD leads to a similar yet small influence. Moreover, DCD can decrease the moment resisted by the rocking wall, while CCD decreases the moment at the upper part but increases the base moment.

(4) The influences of control devices on the dimensionless dynamic responses of flexural-shear beams are dominated by the ratio of natural frequency to excitation frequency. Generally, DCD can sufficiently suppress the interstory drift of rocking wall-frame buildings, and results in significant drift concentration. In contrast, CCD does not clearly reduce the interstory drift, but avoids drift concentration. In the case of real ground motions, both devices are always detrimental to suppress floor acceleration responses, especially DCD. Thus, the reasonable control device should be determined based on the response concerned in the seismic design of rocking wall-frame buildings.

6. Acknowledgements

The supports of the National Natural Science Foundation of China (Grant Nos. 51478086 and 11772079), and the Open Foundation of State Key Laboratory of Disaster Reduction in Civil Engineering (Grant No. SLDRCE17-03) are much appreciated.

7. Copyrights

8. References

[1] Konstantinidis D, Makris N (2005): Seismic response analysis of multidrum classical columns. *Earthquake Engineering & Structural Dynamics*, **34**(10), 1243–1270.

[2] Tung CC (2007): Initiation of motion of a free-standing body to base excitation. *Earthquake Engineering & Structural Dynamics*, **36**(10), 1431–1439.

[3] Vassiliou MF, Makris N (2012): Analysis of the rocking response of rigid blocks standing free on a seismically isolated base. *Earthquake Engineering & Structural Dynamics*, **41**(2), 177–196.

[4] Dimitrakopoulos EG, Paraskeva TS (2015): Dimensionless fragility curves for rocking response to near-fault excitations. *Earthquake Engineering & Structural Dynamics*, **44**(12), 2015–2033.

[5] Ajrab JJ, Pekcan G, Mander JB (2004): Rocking wall–frame structures with supplemental tendon systems. *Journal of Structural Engineering*, **130**(6), 895–903.

[6] Alavi B, Krawinkler H (2004): Strengthening of moment-resisting frame structures against near-fault ground motion effects. *Earthquake Engineering & Structural Dynamics*, **33**(6), 707–722.

[7] Diamantopoulos S, Fragiadakis M (2019): Seismic response assessment of rocking systems using single degree-of-freedom oscillators. *Earthquake Engineering & Structural Dynamics*, **48**(7), 689–708.

[8] Qu Z, Wada A, Motoyui S, Sakata H, Kishiki S (2012). Pin-supported walls for enhancing the seismic performance of building structures. *Earthquake Engineering & Structural Dynamics*, **41**(14), 2075–2091.

[9] Grigorian CE, Grigorian M (2016): Performance control and efficient design of rocking-wall moment frames. *Journal of Structural Engineering*, **142**(2), 04015139.

[10] Grigorian M, Grigorian C (2016): An introduction to the structural design of rocking wall-frames with a view to collapse prevention, self-alignment and repairability. *Structural Design of Tall and Special Buildings*, **25**(2), 93–111.

[11] Grigorian M, Moghadam AS, Mohammadi H (2017): Advances in rocking core-moment frame analysis. *Bulletin of Earthquake Engineering*, **15**(12), 5551–5577.

[12] Miranda E, Akkar SD (2006): Generalized interstory drift spectrum. *Journal of Structural Engineering*, **132**(6), 840–852.

[13] Wu DY, Zhao B, Lu XL (2018): Dynamic behavior of upgraded rocking wall-moment frames using an extended coupled-two-beam model. *Soil Dynamics and Earthquake Engineering*, **115**, 365–377.

[14] Sun TS, Kurama YC, Zhang PZ, Ou JP (2018): Linear-elastic lateral load analysis and seismic design of pin-supported wall-frame structures with yielding dampers. *Earthquake Engineering & Structural Dynamics*, **47**(4), 988–1013.

[15] Makris N, Black CJ (2004): Dimensional analysis of rigid-plastic and elastoplastic structures under pulse-type excitations. *Journal of Engineering Mechanics*, **130**(9), 1006–1018.

[16] Makris N, Black CJ (2004): Dimensional analysis of bilinear oscillators under pulse-type excitations. *Journal of Engineering Mechanics*, **130**(9), 1019–1031.

[17] Makris N, Vassiliou MF (2011): The existence of 'complete similarities' in the response of seismic isolated structures subjected to pulse-like ground motions and their implications in analysis. *Earthquake Engineering & Structural Dynamics*, **40**(10), 1103–1121.

[18] Zhai CH, Jiang S, Chen ZQ (2015): Dimensional analysis of the pounding response of an oscillator considering contact duration. J Eng Mech, **141**(4), 04014138.43. Miranda E, Taghavi S (2005): Approximate floor acceleration demands in multistory buildings. I: formulation. *Journal of Structural Engineering*, **131**(2), 203–211.

[19] Mavroeidis GP, Papageorgiou AS (2003): A mathematical representation of near-fault ground motions. *Bulletin of the Seismological Society of America*, **93**(3), 1099–1131.

[20] Alonso-Rodr ́guez A, Miranda E (2015): Assessment of building behavior under near-fault pulse-like ground motions through simplified models. *Soil Dynamics and Earthquake Engineering*, **79**, 47–58.

[21] Yang DX, Guo GQ, Liu YH, Zhang JF (2019): Dimensional response analysis of bilinear SDOF systems under near-fault ground motions with intrinsic length scale. *Soil Dynamics and Earthquake Engineering*, **116**, 397–408.

